



Carbon Burial in two Greenland Fjords: Exploring the Influence of Glacier Type on Organic Carbon Dynamics

Marius Buydens¹, Emil De Borger¹, Lorenz Meire^{2,5}, Samuel Bodé³, Antonio Schirone⁴, Karline Soetaert⁵, Ann Vanreusel¹, Ulrike Braeckman^{1,6}

¹Marine Biology Research Group, Ghent University, Krijgslaan 281, S8 9000, Gent, Belgium

²Greenland Climate Research Centre, Greenland Institute of Natural Resources, Kivioq 2, 3900 Nuuk, Greenland

³Isotope Bioscience Laboratory (ISOEYS), Ghent University, Coupure Links 653, 9000 Ghent, Belgium

⁴ENEA, Department of Sustainability, Marine Environment Research Centre S. Teresa, Via Santa Teresa 1, 19032 Pozzuolo di Leri, Italy

⁵Royal Netherlands Institute of Sea Research (NIOZ), Department of Estuarine and Delta Systems, Koringaweg 7, P.O. Box 140, 4401, NT, Yerseke, the Netherlands

⁶Institute of Natural Sciences, Operational Directorate Natural Environment, Vautierstraat 29, 1000, Brussels, Belgium

Correspondence to: Marius Buydens (marius.buydens@ugent.be)

Abstract. Fjord systems are crucial for the burial and long-term storage of organic carbon (OC), contributing significantly to global blue carbon sequestration. Despite their importance, Greenland's fjords remain underrepresented in global carbon budgets, even though accelerated melt of the Ice Sheet alters these ecosystems through increased freshwater discharge and iceberg calving, ultimately leading to glaciers retreating inland. This study compares organic carbon burial rates (OCBRs) in two neighbouring Greenland fjords—Nuup Kangerlua, influenced by marine-terminating glaciers (MTGs), and Ameralik, dominated by land-terminating glaciers (LTGs)—to explore the effects of both types of glaciers on sediment carbon dynamics. Since subglacial discharge-driven upwelling in Nuup Kangerlua (MTG) has been shown to support higher summer phytoplankton blooms, we expected higher sediment organic carbon content and burial in this MTG fjord. However, our observations show higher OC content in sediments of Ameralik's (LTG) outer and mid fjord section and a similar OCBR in both fjords. This unexpected finding may be linked to differences in pelagic grazing pressure, organic carbon transport, and sediment preservation mechanisms. The findings call for further research to unravel the complex interactions between primary production, organic carbon transport, and preservation processes in different glacial fjord systems.

1 Introduction

Fjord systems play a crucial role in burial and long-term storage of organic carbon, contributing to approximately a tenth of the annual blue carbon burial (Smith et al., 2015). In the Northern hemisphere, carbon content and burial in fjord sediments have mainly been studied in Alaska (Cui et al., 2016a), Scotland and Ireland, (Smeaton et al., 2016; Smeaton and Austin, 2017; Smeaton and Austin, 2019; Smeaton et al., 2021), Norway (Faust and Knies, 2019; Włodarska-Kowalczyk et al., 2019), Sweden (Placitu et al., 2024; Watts et al., 2024) and Svalbard (Kuliński et al., 2014; Koziorowska et al., 2018; Zaborska et al., 2018; Włodarska-Kowalczyk et al., 2019).



Nevertheless, despite the prevalence of fjords along Greenland's extensive coast, a notable gap remains in their representation in global carbon budgets (Smith et al., 2015). Moreover, Greenland harbours the only remaining Arctic ice sheet since the last
35 glacial period, which plays a key role in regulating Earth's climate and sea-level. The current accelerated melting of the Greenland Ice Sheet (King et al., 2020; Greene et al., 2024), driven by climate change, has far-reaching global implications and is altering fjord systems through increased freshwater discharge and iceberg calving (Calleja et al., 2017; Catania et al., 2020; Kanna et al., 2022).

40 Glaciers in polar regions either calve directly into the ocean (so called "marine-terminating glaciers", further referred to as MTGs) or terminate inland, discharging into lakes or the ocean via meltwater rivers ("land-terminating glaciers", LTGs). Fjords, inundated relict valleys carved out during previous glacial periods, often serve as channels through which these glaciers and meltwater rivers reach the ocean. Meltwater percolates down the cracks and crevices of glaciers to ultimately form sub-glacial rivers at their base (Chu, 2014). Since MTGs terminate in the ocean, this sub-glacial meltwater rises up from the bottom
45 of the glacier within the fjord basin entraining nutrients present in deeper water layers (Hopwood et al., 2020 and references therein). This upwelling water mass replenishes essential nutrients in the surface waters, crucial for sustaining phytoplankton proliferation beyond the initial spring bloom phase. This extended bloom, running into the summer months may potentially lead to increased organic carbon production within the fjord ecosystem (Kanna et al., 2022; Meire et al., 2023). Conversely, fjords receiving meltwater from LTGs lack this mechanism of upwelling, leading to a depletion of nutrients following the
50 spring bloom period, resulting in substantially lower primary production in summer (Meire et al., 2017, 2023). Consequently, the carbon dynamics in LTG-dominated fjords may differ significantly from those observed in MTG-dominated fjords.

An important characteristic of fjord systems that enhances their capacity as carbon sinks is an elevated sedimentation rate, driven by their proximity to glaciers and rivers, along with the steep terrain of their watersheds (Syvitski, 1987). However,
55 sedimentation rate alone is not the sole determinant of effective carbon burial (Bianchi et al., 2020). In general, the effectiveness of trapping organic carbon varies among fjords and depends on (1) the productivity of the fjord waters, particularly phytoplankton growth, as well as terrestrial vegetation growth in the catchment, both of which are influenced by climate (e.g. fjord categories described in Włodarska-Kowalczyk et al., 2019), (2) factors affecting the settlement of organic carbon (OC) to the fjord's bottom sediments (e.g. fjord geomorphology and current dynamics) (Gilbert et al., 2002; Faust and
60 Knies, 2019; Watts et al., 2024) and (3) factors limiting the degradation of settled OC, among which the refractory nature of OC (Koziorowska et al., 2015; Zaborska et al., 2018), sedimentation rate (Watts et al., 2024) and bottom water redox conditions (Hinojosa et al., 2014).

Findings from the limited number of biogeochemical studies focusing on Greenland fjords have sparked speculation that
65 enhanced primary production observed in MTG-dominated fjords, driven by the upwelling effect, may lead to increased carbon sequestration in fjord sediments compared to LTG-influenced fjord systems (Meire et al., 2017; Meire et al., 2023; Stuart-Lee



et al., 2023). However, there is limited data from Arctic fjords to test this hypothesis. In Svalbard, a lower OC content has been observed in the surface sediments of a LTG-fed fjord compared to two MTG-impacted fjord systems (Laufer-Meiser et al., 2021). In contrast, another study conducted in Svalbard reported a higher OC content in the surface sediments of a LTG-
70 compared to a MTG-influenced fjord (Koziorowska et al., 2015). While the first study ascribed the observed pattern to the glacier-driven upwelling effect, the second study attributed the higher OC content to the higher proportion of terrestrially-derived organic matter versus the more degradable marine organic matter. A study comparing organic carbon burial rates (OCBR) in Arctic fjords stated that high Arctic fjords with limited glacial activity and a short phytoplankton growth period sequester lower amounts of carbon in the sediments compared to Arctic fjords with “active” glaciers and a relatively longer
75 phytoplankton growth period (Włodarska-Kowalczyk et al., 2019).

This study aims to improve our understanding of carbon burial processes in Greenland fjord systems and provide insights that may refine estimates of their contribution to carbon burial at regional scales. In addition, we seek to gain insights in the influence of different types of Greenland fjord systems, more specifically in terms of MTG or LTG discharge influence. This
80 knowledge is crucial for developing a comprehensive understanding of how climate change may impact the long-term carbon storage capacity of Greenland fjord systems and the potential related feedback effects on global climate systems.

Therefore, we compared carbon storage and burial in two neighbouring, sub-Arctic fjord systems which both feature a sill at their entrance and are subjected to similar offshore currents and similar geology in their catchments, but have a different glacier
85 influence (MTG-dominated vs. LTG-dominated fjords).

2 Materials and methods

2.1 Study area

The two fjord systems are situated in the sub-Arctic coastal region of Southwest Greenland. Covering an area of 2,013 km², Nuup Kangerlua (formerly known as Godthåbsfjord) forms, with its many side branches, the largest fjord system of West
90 Greenland (Mortensen et al., 2018). The main branch is ~190 km long. Three marine-terminating glaciers and three meltwater rivers discharge into the fjord (Mortensen et al., 2011; Fig. 1). The land-terminating glaciers release 7.5 ± 2.1 km³ yr⁻¹ of freshwater into the fjord system, while the marine-terminating glaciers supply 18.4 ± 5.8 km³ yr⁻¹ of freshwater in addition to 7–10 km³ yr⁻¹ of solid ice discharge (Van As et al., 2014; Langen et al., 2015). The seafloor morphology comprises two consecutive sills at the fjord entrance and a third sill located in the inner fjord area in front of the termini of the two
95 innermost MTGs (Mortensen et al., 2011; Fig. 1). Inflow of dense coastal waters renews basin water masses in the main fjord basin usually from November until April (Mortensen et al., 2011, 2014, 2018). Bottom water temperatures are between 1.5 and 2°C (Mortensen et al., 2011).



Ameralik is situated south of Nuup Kangerlua, and has a length of around 75 km and a surface area of 400 km² (Stuart-Lee et al., 2023). The fjord receives most of the freshwater runoff from a meltwater river (Naujat Kuat) draining an inland glacier. Overeem et al. (2015) measured in 2012 a discharge of 0.78 km³ yr⁻¹ of Naujat Kuat into the fjord. A large sill is situated at the mouth of Ameralik and rises to 110 m water depth (Stuart-Lee et al., 2021). Being more than twice as shallow compared to the entrance sills in Nuup Kangerlua, the sill restricts inflow of relatively warmer and more saline sub-polar mode water (SPMW), resulting in relatively lower bottom water temperatures of ~0–1°C (spring and summer 2019 data; Stuart Lee et al., 2021). The seafloor geomorphology behind the sill consists of a series of basins with the deepest and more extensive basin situated about 20 km inwards from the main sill. Within this basin, the bathymetry plummets to a water depth of approximately 730 m.

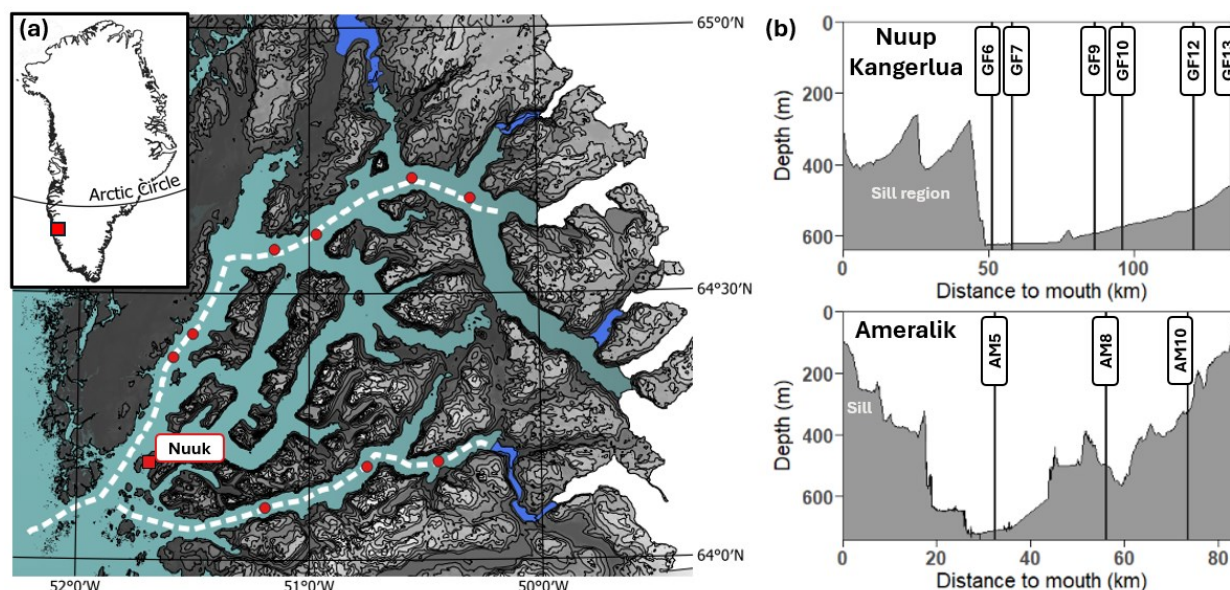


Figure 1: A. Red dots mark the locations of the sampled stations in Nuup Kangerlua (upper fjord; from mouth to head: GF6, GF7, GF9, GF10, GF12 & GF13) and Ameralik (lowermost fjord; from mouth to head: AM5, AM8 & AM10). Areas indicated in blue represent the main river valleys and deltas. Glaciers and Ice Sheet are indicated in white. White dashed lines shows the transects of the depth profiles. B. Water depth profiles along-axis (white dashed lines) Nuup Kangerlua (top) and Ameralik (bottom).

2.2 Sediment sampling

Two field campaigns were organized, one in summer 2021 and one in spring 2022. Sediment samples were taken from the research vessels *Polar Diver* (2021) and *Avataq* (2022). A UWITEC multicorer (UWITEC GmbH, Austria) was deployed to sample the seafloor and included three core liners of 60 cm long with an inner diameter of 8.6 cm. Stations were located along the main axis of both fjords (Fig. 1). No successful deployments could be carried out at the sill areas situated at the mouth area of both fjords due to the high abundance of gravel. Sampled stations are therefore located behind the sills, within the fjord basin. Although the mouth areas of both fjords could not be sampled, we divided each fjord basin into “outer,” “mid,” and



“inner” sections for clarity. Throughout the text, the terms “outer,” “mid,” and “inner” refer to specific station locations. For Nuup Kangerlua, the “outer” area corresponds to stations GF6 and GF7, the “mid” area to GF9 and GF10, and the “inner” area to GF12 and GF13. In Ameralik, the “outer,” “mid,” and “inner” fjord areas correspond to stations AM5, AM8, and AM10, respectively.

2.2.1 Solid phase sampling

At each station, three deployments were carried out for granulometry, pigment, TOC and TN analysis ($n = 3$) and one deployment for porosity and ^{210}Pb analysis ($n = 1$) and for stable isotope analysis of C and N ($n = 1$; in 2022). Due to the more exploratory approach of the 2021 campaign, less stations and parameters were sampled compared to 2022 (Table 1). The retrieved sediment was sliced into 1 cm thick slices down to 10 cm sediment depth. Sediment intended to derive sediment accumulation rates (^{210}Pb analysis) was further sliced beyond 10 cm in intervals of 2 cm until the end of the core (ranging from 10 to 44 cm sediment). All samples were stored at -20°C , except for sediment samples intended for pigment analysis, which were stored at -80°C .

Table 1 Sampling dates, coordinates, water depth, and bottom water temperatures (BWT) of sampled stations in Nuup Kangerlua (Godthåbsfjord; GF) and Ameralik (AM).

Station	Date(s) sampled	Longitude (N)	Latitude (W)	Depth (m)	BWT ($^\circ\text{C}$)	
					2021	2022
GF13	31/05/2022	$64^\circ 40.8$	$50^\circ 17.3$	476	1.4742	1.4135
GF12	31/08/2021 20/05/2022	$64^\circ 42.9$	$50^\circ 32.8$	531	1.4135	1.347
GF10	31/08/2021	$64^\circ 36.6$	$50^\circ 57.5$	570	1.3239	0.8074
GF9	24/05/2022	$64^\circ 33.0$	$51^\circ 0.9$	626	1.228	0.6737
GF7	01/09/2021 20/05/2022	$64^\circ 25.5$	$51^\circ 3.4$	630	1.2908	0.6387
GF6	30/08/2021	$64^\circ 22.0$	$51^\circ 0.4$	630	1.2791	0.6185
AM10	02/09/2021 18/05/2022	$64^\circ 11.0$	$50^\circ 25.9$	350	0.4943	0.4452
AM8	18/05/2022	$64^\circ 10.4$	$50^\circ 45.3$	488	0.5925	0.5571
AM5	03/09/2021 24/05/2022	$64^\circ 05.7$	$51^\circ 11.3$	730	0.5597	0.59



2.3 Solid phase sample analysis

Grain size distribution was determined on oven-dried samples (at 60 °C for 48 h) applying the laser diffraction method using a Malvern Mastersizer 2000 with Hydro 2000S module (0.02–2000 mm size range). Results were categorized in clay (<4 mm), silt (4–63 mm), and sand (63–500 mm) fractions conform Wentworth scale classification (1922). Porosity was obtained by dividing the porewater volume by the wet sediment volume. Samples were dried and homogenized, then analyzed for total sedimentary carbon (TC) and total nitrogen (TN). After decalcification with 37 % HCl, total organic carbon (TOC) was also measured. All measurements were conducted using a Flash 2000 NC Sediment Analyzer (Interscience). From these data, the molar CN ratios were calculated and inorganic carbon (IC) was determined by subtracting TOC from TC. To investigate the origin of the organic matter (see further), stable isotope composition ($\delta^{13}\text{C}$ and $\delta^{15}\text{N}$) was measured with an elemental analyzer (Thermo Flash EA1112 element analyzer) coupled to an isotope ratio mass spectrometer (Thermo Finnigan Delta V, IRMS). To explore how glacier type affects marine primary productivity and whether and how it is incorporated in the sediment, we additionally measured, for each sediment slice, the content of chlorophyll-a (Chl-a) and of its degradation products (pheophorbide-a, and pheophytin-a, pheophorbide-a like, and pheophytin-a like following Wright and Jeffrey (1997). These different pigments were determined by the response factor of standard pigments as described by Van Heukelem and Thomas (2001). The ratio of Chl-a to Chloroplastic Pigment Equivalent (CPE, comprising the sum of all aforementioned pigments) was used as a proxy for the “freshness” of photosynthetically produced organic matter.

2.3.1 Calculation of marine organic carbon fraction

Stable isotope composition in addition to C:N ratios of settled organic matter in fjord sediments has been used in multiple studies to estimate the proportion of marine versus terrestrially derived OM (Koziorowska et al., 2015; Smeaton & Austin, 2017; Faust and Knies, 2019). However, the use of solely stable isotopes can render an overestimation of marine OM as eroded and reburied fossil carbon from rocks (petrogenic carbon) display $\delta^{13}\text{C}$ values within the range of recent marine OM masking a marine fossil provenance (Burdige, 2007; Cui et al., 2016b; Wang et al., 2024). The bedrock of the catchments of both fjords is predominantly made up of Precambrian orthogneisses, granodiorites and granites. Potential sources of petrogenic carbon like meta-sedimentary rocks occur, but are rather rare in the catchment areas (<0.1 % of exposed bedrock) (Næraa et al., 2014). Therefore, it is reasonable to assume that the input of ancient marine carbon is likely to be limited. The fraction of OC derived from terrestrial C was calculated following the formula of Thornton and McManus (1994):

$$OC_{\text{terrestrial}} = \frac{\delta^{13}\text{C}_i - \delta^{13}\text{C}_M}{\delta^{13}\text{C}_T - \delta^{13}\text{C}_M} \quad (1)$$

and

$$OC_{\text{marine}} = 1 - OC_{\text{terrestrial}}, \quad (2)$$

where $\delta^{13}\text{C}_i$ represents the surface sediment values (0–2 cm) of $\delta^{13}\text{C}_{\text{org}}$ of each sample, $\delta^{13}\text{C}_M$ is the marine end-member and $\delta^{13}\text{C}_T$ is the terrestrial end-member. These end-members were adopted from Faust and Knies (2019): -19.3‰ and -26.5‰ vs.



V-PDB-LSVEC, for the marine and terrestrial end-member, respectively. These end-members were derived from Northern and Mid-Norway fjord sediments and agree with western Barents Sea sediments (Knies and Martinez, 2009; Faust and Knies, 2019) and Svalbard fjord sediments (Winkelman and Knies, 2005).

2.4 ^{210}Pb and ^{137}Cs analysis

Lead-210 dating of the sediment was done using HPGe gamma ray spectroscopy (diameter: 101.6 mm, height 134.9 mm, carbon-epoxy window, model BE5030-7500SL-RDC-4, Canberra, Asse, Belgium). The dried and grinded sediment samples were packed into aluminium tins with calibrated geometries of 35 ml, 60 ml or 120 ml, depending on the amount of dried sediment available, and left for > 21 days after sealing allowing ingrowth equilibration of the ^{226}Ra with the proxies used to estimate its activity (^{214}Pb and ^{214}Bi) (Brenner et al. 2004). When tins could not be filled entirely, the headspace was measured accurately, and an empirical model per geometry was used to correct for change in efficiency. The measurement of ^{210}Pb activity was done using its 46.5-KeV gamma peak as described by Cutshall et al. (1983). The contribution of “supported” ^{210}Pb was assessed by estimating the ^{226}Ra activity from the average of the ^{214}Pb (at 295.2 and 351.9 keV) and ^{214}Bi (at 609.3 keV) activities. Supported ^{210}Pb was then subtracted from the total ^{210}Pb for each depth interval to determine “excess” ^{210}Pb ($^{210}\text{Pb}_{\text{xs}}$). Additionally, ^{137}Cs levels were determined through gamma spectroscopic measurement of its 661.7-KeV gamma peak.

2.4.1 Organic carbon burial rate constant

Log transformed $^{210}\text{Pb}_{\text{xs}}$ activities were plotted against the cumulative dry mass depth (g cm^{-2}) of the sediment per station. Sedimentation rates at stations GF9, GF7, AM8 and AM5 were determined using the constant rate of supply model (CSR) (Appleby, 2001), as a clear ^{137}Cs peak was measured at these stations (Fig. A1). For the stations GF13, GF12, GF10, AM10 and GF6, the sediment mass accumulation rate (MAR, $\text{kg solids cm}^{-2} \text{ yr}^{-1}$) was derived from the slope of the linear regression according to the CF:CS model (Constant Flux:Constant Sedimentation) (Sanchez-Cabeza & Ruiz-Fernández, 2012). The bulk sediment accumulation rate (SAR, mm yr^{-1}) was calculated by dividing MAR by the average bulk density of the sediment per station. The organic carbon burial rate (OCBR) per station was determined using the MAR and the TOC content at the deepest sediment layer in common for all sediment cores (9–10 cm sediment interval depth). No bioturbated or mixed upper layer was observed in the profiles.

2.5 Statistical analysis

We examined differences between the two fjords and between stations in terms of sedimentary TOC and TN content, C/N ratio, Chl-a content and Chl-a:CPE ratio from the upper 2 cm sediment surface and the average of the 10 cm sediment column.



Data from summer (2021) and spring (2022) were combined and treated as replicates, as the difference between the two seasons was insignificant. As a consequence, stations GF12, GF10, GF7, AM10 and AM5 have six replicates since they were sampled in both seasons, while the other stations have three replicates as those stations were only sampled during spring 2022 (Table 1). Statistical analyses were performed using one-way ANOVA. Welch's ANOVA was applied when variances were unequal, and the Kruskal-Wallis test was used when normality assumptions were violated. For significant results, post hoc comparisons were made using Tukey's test, Games-Howell test, or Dunn's test, depending on the initial method. Results are reported as means \pm standard deviation. Statistical analyses were performed in R (R Core Team, 2023) using the car, rstatix and FSA packages (Fox and Weisberg, 2019; Kassambara, 2023; Ogle et al., 2023).

3 Results

3.1 Solid phase parameters

The median grain size ($d_{0.5}$) was situated in the silt fraction for all stations, though AM5, AM8 and the top 2 cm of GF7 displaying medium-sized silt, while all other stations are situated in the very fine to fine silt class (Fig. 2). In Nuup Kangerlua, the median grain size ($d_{0.5}$) shows a clear spatial pattern from the inner to the outer fjord (Fig. 2). At the inner stations (GF13 and GF12), the grain size remains relatively small ($< 20 \mu\text{m}$) and consistent with depth, reflecting a stable depositional environment dominated by fine particles. Moving to the mid-fjord stations (GF10 and GF9), there is a slight increase in grain size, though still within the fine-silt range, indicating limited hydrodynamic influence. At the outer stations (GF7 and GF6), the grain size increases further to medium-sized silt and varies with depth, suggesting the deposition of coarser sediments near the fjord mouth due to stronger currents and more dynamic conditions.

In Ameralik, a similar trend is observed (Fig. 2). The inner station (AM10) shows small, uniform grain sizes comparable to those at the inner stations in Nuup Kangerlua. At the mid-fjord station (AM8), the grain size increases slightly, reflecting a subtle shift in depositional energy. The outer station (AM5) exhibits the largest grain sizes, with noticeable variability at depth, indicating more pronounced hydrodynamic sorting and energy fluctuations in this area.

Porosity and dry density fluctuated along the sediment depth gradient without a clear trend, except for station GF10, where porosity decreased and dry density increased with depth.

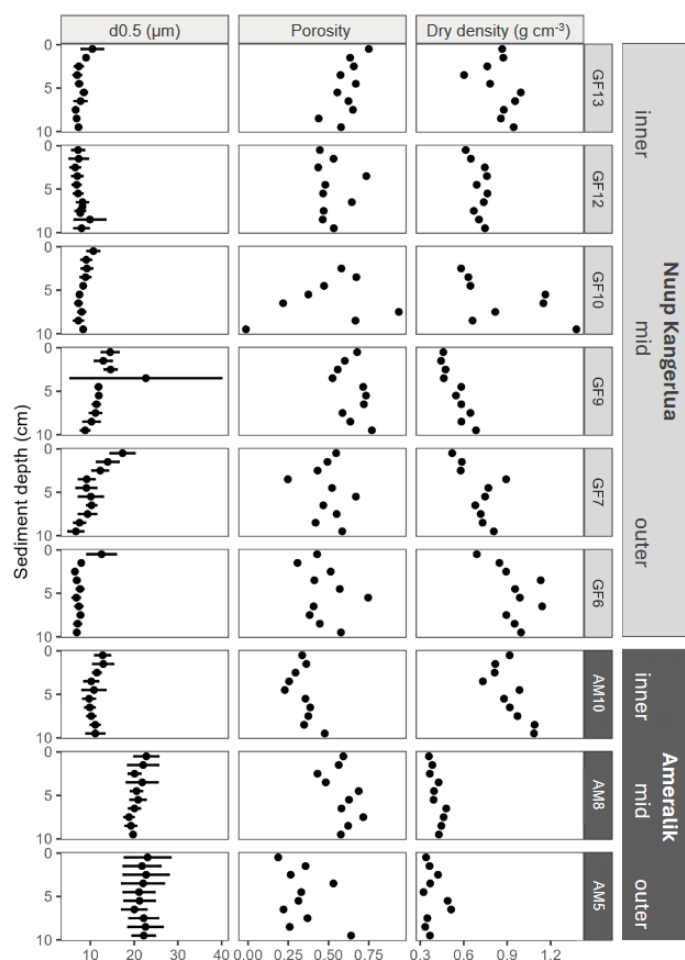


Figure 2: Sediment profiles of median grain size (μm), porosity and dry density (g cm^{-3}) of Nuup Kangerlua (GF stations) and Ameralik (AM stations). Error bars represent SD ($n = 3$ for GF6, GF9, GF13 and AM8 and $n = 6$ for GF7, GF10, GF12, AM5 and AM10). Only one replicate for porosity and dry density.

In Ameralik, we observed a distinct increasing trend in the surface 2 cm sediments from the inner fjord to the mid-fjord stations for TOC, TN, Chl-a content, and the Chl-a:CPE ratio. The only exception was the C:N ratio, which decreased from the inner to the mid-fjord, and then remained relatively constant (Fig. 3). In Nuup Kangerlua, the pattern was more variable. TOC, TN, and Chl-a content rose from the inner fjord towards the mid-fjord stations, peaking at GF7 and GF9, but then declined at GF6, near the outer fjord (Fig. 3). Unlike Ameralik, the Chl-a:CPE ratio in Nuup Kangerlua showed fluctuations along the fjord axis, without a consistent trend. Overall, station AM5, located in the deepest part of the main basin of Ameralik, displayed the highest (Welch's ANOVA, $p < 0.05$) Chl-a ($16.4 \pm 2.0 \mu\text{g g}^{-1} \text{DM}$) and CPE ($45.9 \pm 7.1 \mu\text{g g}^{-1} \text{DM}$) content, as well as the highest Chl-a:CPE ratios (0.36 ± 0.04) of the top 2 cm surface sediments compared to all other sampled stations of both fjords (Fig. 3).



In addition, both outer and mid stations of Ameralik displayed the highest TOC values (AM5: 2.1 ± 1.5 %; AM8: 1.6 ± 0.1 %) within the upper 2 cm sediment, which were significantly higher (Welch's ANOVA, $p < 0.05$) than those observed in inner fjord station AM10 and all stations in Nuup Kangerlua (values ranging from 0.1 to 1.3 %).

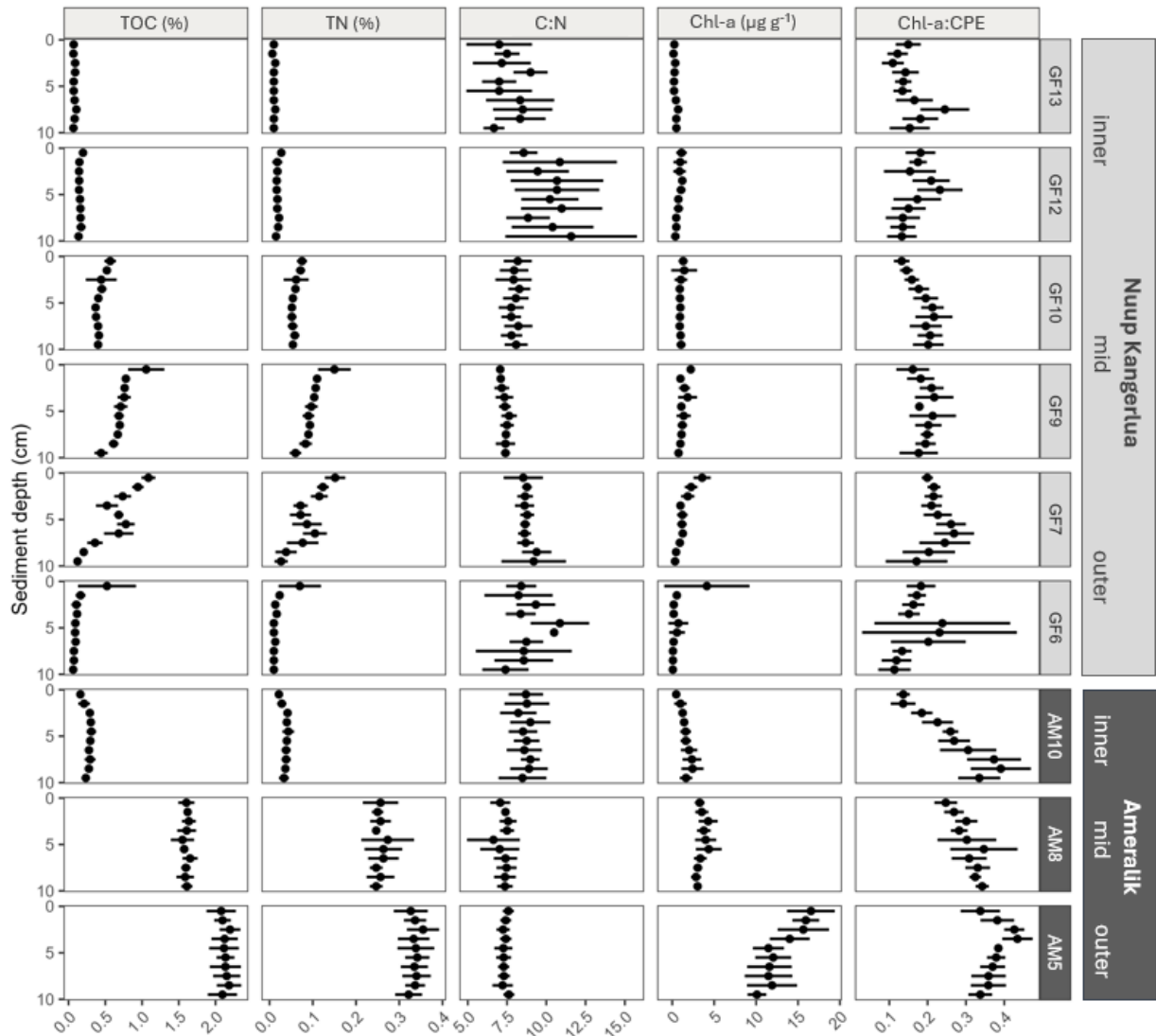


Figure 3: Vertical sediment profiles depicting TOC and TN (%), molar C:N ratios and Chl-a ($\mu\text{g/g DM}$) of the upper 10 cm sediment of Nuup Kangerlua (GF stations) and Ameralik (AM stations). Error bars represent SD ($n = 3$ for GF6, GF9, GF13 and AM8 and $n = 6$ for GF7, GF10, GF12, AM5 and AM10).



Apart from GF13, the organic carbon in all stations within both fjords displayed $\delta^{13}\text{C}$ values characteristic for marine algae (-22.4 to -20.7 ‰). While the $\delta^{13}\text{C}$ value fluctuated widely at GF13 ranging from -26.3 to -23.8 ‰, while $\delta^{15}\text{N}$ consistently increased with sediment depth from 5.7 to 12.2‰ (Fig. A2). The more depleted $\delta^{13}\text{C}$ values at this station suggest relatively more mixing with terrestrial OM, while $\delta^{15}\text{N}$ levels are more indicative of a marine origin, since values are well above 1 ‰ and no intensive agriculture exists in the region (Harris and Elliot, 2019; Fig. 4). Levels of $\delta^{13}\text{C}$ in the upper 2 cm slightly increased from inner to outer stations within Nuup Kangerlua indicating an increasing marine influence in terms of organic carbon composition towards the outer fjord area. In Ameralik, the least depleted $\delta^{13}\text{C}$ signatures were observed in AM8.

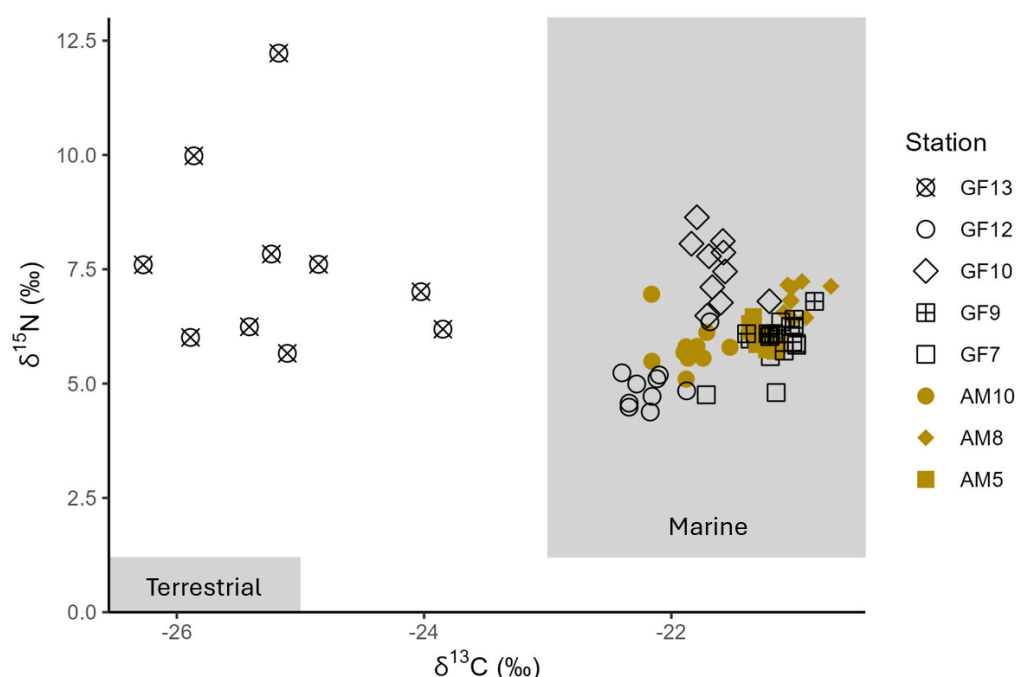


Figure 4: $\delta^{13}\text{C}$ (‰ deviations from V-PDB) values plotted against $\delta^{15}\text{N}$ (‰ deviations from air) values of the POM present in the sediment for the different station of Ameralik (colored) and Nuup Kangerlua (open symbols). Typical marine and terrestrial ranges of $\delta^{13}\text{C}$ and $\delta^{15}\text{N}$ are indicated with rectangles following Zaborska et al. (2018).

3.2 Organic carbon burial rates

Sediment mass (MAR) and volume accumulation rates (SAR) roughly showed an increasing trend towards the inner fjord in Nuup Kangerlua. In Ameralik, MAR and SAR are also higher in the inner compared to the outer station, with minimum values

in the mid station (Table 2). Burial rates of organic carbon increased towards the fjord head in Nuup Kangerlua until mid-fjord station GF10 where it reached the maximum observed rate ($29.4 \text{ g OC m}^{-2} \text{ yr}^{-1}$). Following station GF12 revealed a marked drop in OCBR ($9.6 \text{ g OC m}^{-2} \text{ yr}^{-1}$), whereafter high OCBR reappear in GF13 ($27.5 \text{ g OC m}^{-2} \text{ yr}^{-1}$). In Ameralik, an opposite pattern unfolded with maximum OCBR in AM5 ($24.7 \text{ g OC m}^{-2} \text{ yr}^{-1}$) and minimum rate in inner fjord AM10 ($9.9 \text{ g OC m}^{-2} \text{ yr}^{-1}$).

Table 2. Mass sediment accumulation rate (MAR), bulk sediment accumulation rate (SAR) and organic carbon burial rate (OCBR) per station. Stations are situated from mid fjord towards the head (inner): “GF” denotes Nuup Kangerlua and “AM” Ameralik.

Station	MAR ($\text{kg m}^{-2} \text{ yr}^{-1}$)	SAR (mm yr^{-1})	OCBR ($\text{g m}^{-2} \text{ yr}^{-1}$)
GF13	14.1 ± 3.5	15.0 ± 3.7	27.5 ± 8.3
GF12	5.9 ± 1.0	7.1 ± 1.2	9.6 ± 1.7
GF10	7.0 ± 0.1	8.3 ± 1.1	29.4 ± 4.0
GF9	3.4 ± 0.1	5.1 ± 1.4	19.1 ± 5.2
GF7	2.6 ± 0.1	3.5 ± 1.3	6.5 ± 2.7
GF6	1.8 ± 0.1	1.9 ± 0.8	1.5 ± 0.6
AM10	4.0 ± 2.8	5.2 ± 2.0	13.1 ± 5.0
AM8	1.1 ± 0.0	2.4 ± 0.0	17.2 ± 0.3
AM5	1.1 ± 0.0	2.9 ± 0.3	23.9 ± 2.3

4 Discussion

The OC content in the sediments of Nuup Kangerlua and Ameralik fall within the range of other (sub) Arctic fjord sediments (Fig. 5A). In addition, the OCBR values are representative for Arctic fjords (Włodarska-Kowalczyk et al., 2019). In terms of fresh organic matter, we found an average Chl-a content in Nuup Kangerlua’s sediments which was slightly below the typical range observed in other North Atlantic fjords (Włodarska-Kowalczyk et al., 2019). In contrast, Ameralik exhibited an average



260 Chl-a concentration nearly three times higher than the maximum values reported for Svalbard fjords (Włodarska-Kowalczyk et al., 2019). This elevated average is largely driven by the exceptionally high Chl-a content observed at station AM5.

We expected higher OC content and OCBRs in Nuup Kangerlua compared to Ameralik, as MTGs present in Nuup Kangerlua increase nutrient upwelling, allowing primary productivity to extend over longer periods. Indeed, at the start of the productive season (April, May), Stuart-Lee et al. (2023) and Meire et al. (2023) noted comparable primary productivity in Nuup Kangerlua and Ameralik. Yet, with increasing meltwater discharge, a summer bloom was observed in Nuup Kangerlua which led to a greater overall phytoplankton biomass compared to Ameralik (Stuart-Lee et al., 2023; Meire et al., 2023). Surprisingly, we found a higher OC content in sediments of outer and mid fjord stations AM5 and AM8 in Ameralik compared to Nuup Kangerlua. These findings are supported by observations from a gravity core sampled nearby station AM5, which also revealed similar elevated carbon content in the sediment (Møller et al., 2006).

270 When comparing datasets from other fjords (Thamdrup et al., 2007; Cui et al., 2016b; Faust and Knies, 2019; Włodarska-Kowalczyk et al., 2019; Laufer-Meiser et al., 2021), LTG systems and non-glaciated regions appear to have surface sediments with OC content comparable to those in MTG systems (Fig. 5A). This suggests that factors beyond glacial influence play a significant role in controlling the degree of benthic-pelagic coupling. Specifically, the presence of MTGs does not inherently result in higher OC accumulation within sediments compared to systems without subglacial upwelling. However, variations in

275 MARs may dilute OC concentrations with inorganic material, potentially skewing these observations. Additionally, higher TOC in surface sediments does not automatically equate to more efficient OC burial.

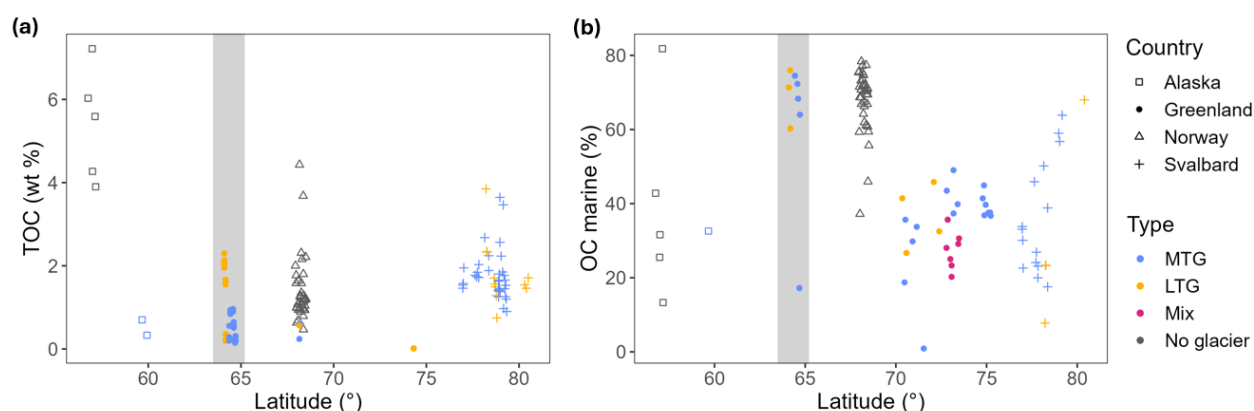


Figure 5: A. TOC content of surface sediments along latitude. **B.** Fraction of TOC of marine origin along latitude. Both figures display data from fjords located in high latitude countries: Alaska, Greenland, Norway and Svalbard. The grey band constraints the Greenland fjords investigated in this study. Data indicated in blue and red represent Marine terminating-glacier (MTG) and land terminating-glacier (LTG)-influenced fjord systems, respectively. The mixed type represents fjords where the dominance of MTG(s) vs LTG(s) on the fjord's hydrology could not be differentiated



from literature or satellite images. Fjord data illustrated in grey represent fjords hosting no major glaciers within their catchments. Both graphs were created following and updating the example of Faust and Knies (2019).

In what follows, we try to substantiate these apparent contradictory results by considering organic carbon, lability, the biogeochemical context, and variations in the export mechanisms between different fjords. Furthermore, recent findings on pelagic grazing pressures in both fjords highlight the role of food-web dynamics in carbon burial dynamics.

280

4.1 Enhanced OC preservation

An important clue in resolving the observed patterns can be found in the deepest part of Ameralik's basin. There, at station AM5, we measured a higher Chl-a content combined with higher Chl-a:CPE ratios compared to Nuup Kangerlua, which points to an enhanced preservation of fresh organic matter within these sediments. The Chl-a content remains elevated throughout the entire 10 cm sediment profile and is consistent between spring and summer data. A difference in timing of the onset of the phytoplankton bloom between the two fjords, as previously observed (Stuart-Lee et al., 2023), could have led to an earlier build-up of pigments at the seafloor of Ameralik compared to Nuup Kangerlua at the time of sampling. However, the relatively elevated values throughout the 10 cm sediment profiles and the consistency between spring and summer data exclude such sampling bias. In Svalbard, Koziorowska et al. (2015) also observed higher OC content in the surface sediments of a LTG-influenced fjord versus a MTG-impacted fjord. The LTG-fed fjord appeared to receive a higher fraction of terrestrial OC, which tends to be more resistant against degradation compared to marine OC (Koziorowska et al., 2015). Yet, in our case, the sediment stable isotope composition and C:N ratios of both fjords reflect OC of predominantly marine origin in both fjords, likely due to the limited vegetation and similar catchment geology consisting of orthogneisses, granodiorites and granites rather than organic-rich sedimentary rocks (Næraa et al., 2014) (Fig. 4; Fig. 5B). An exception is inner station GF13 in Nuup Kangerlua, which displayed $\delta^{15}\text{N}$ and C:N ratios of marine signature, though depleted $\delta^{13}\text{C}$ values indicative of a terrestrial provenance.

Therefore, if a different degree in organic matter preservation occurs between the two fjords, it has to be linked to environmental conditions rather than the nature of the OC itself. Metal shielding, particularly the association of OC with iron or manganese, may be another factor influencing the preservation of sedimentary OC. Reactive iron minerals such as iron- and manganese(oxyhydr)oxides preferentially bind to marine organic matter, forming complexes that enhance the protection of OC from microbial degradation and remineralization (Faust et al., 2022; Moore et al., 2023). Such carbon-iron and -manganese interactions have been found to persist over geological timescales, thereby enhancing long-term carbon sequestration (Faust

300



et al., 2021; Moore et al., 2023; Wang et al., 2024). Indeed, the Greenland Ice Sheet acts as a major source of Fe and Mn to its surrounding fjords through both subglacial and glacial river discharge (Bhatia et al., 2013; Hawkings et al., 2014; 2020).
305 Studies conducted in Nuup Kangerlua and Ameralik revealed that both fjords receive substantial amounts of Fe and Mn from (sub)glacial river inflow, which appears to be captured within the fjord basin rather than being exported offshore (Hopwood et al., 2016; Krause et al., 2021; van Genuchten 2021; 2022). Higher Fe and Mn concentrations were measured in the surface waters of inner Ameralik compared to Nuup Kangerlua, but similar concentrations appeared towards the outer area of both fjords (Krause et al., 2021; van Genuchten 2022). However, no information is available on the concentration of solid Fe and
310 Mn particles or derived complexes in the basin sediments. Moreover, differences in the balance and interplay between sedimentation rate, influx of organic matter and Fe and Mn species, the reactivity of Fe and Mn and the depth of sulphate reduction can play a role in differences in preservation of OC (Wehrmann et al. 2014; Michaud et al., 2020; Herbert et al., 2021; Laufer-Meiser et al., 2021). This complexity, however, goes beyond the scope of this study. Hence, it is not clear if metal shielding plays a role in elevated OC and Chl-a content in Ameralik's deep basin sediments.
315 The distinct geomorphology of Ameralik and Nuup Kangerlua, particularly their differing sill depths, likely shapes bottom water temperatures and may influence organic matter preservation within the fjords. Both fjords have no anoxic deep water masses and bottom water renewal occurs every one to two years (Mortensen, 2011; Stuart-Lee et al., 2021), but bottom water temperature differs. Ameralik's shallower sill depth (~110 m) compared to Nuup Kangerlua (~200 m) restricts the inflow of warmer, saltier coastal waters (Stuart-Lee et al., 2021). As a result, Ameralik's deep waters (below 400 m) are around zero
320 degrees and about one to two degrees colder than in Nuup Kangerlua (Stuart-Lee et al., 2021), which may cause the observed higher pigment preservation in AM5.

4.2 OC transport dynamics

325 In addition to potential differences in organic matter preservation, lateral transport can also play a role in shaping the spatial distribution of OC across the seafloor. In Nuup Kangerlua, a weak along-fjord gradient in sedimentary TOC, TN, and Chl-a content suggests a dynamic current regime that may facilitate OC redistribution. Meire et al. (2023) reported a threefold higher primary production rate at station GF10 compared to AM10 due to the summer bloom. Yet, we observe that this higher productivity did not translate into significant differences in sedimentary Chl-a and TOC content between these stations.
330 Although it must be noted that both parameters were relatively higher (although not significantly) at GF10 compared to AM10 and that TOC and Chl-a content at GF10 may have been diluted by the observed higher MAR.

Nuup Kangerlua's estuarine and subglacial circulations, which become most active during the melt season, may enhance OC export from the inner fjord to outer areas (Mortensen et al., 2011; 2014; Juul-Pedersen et al., 2015). Despite this potential for export in the surface waters, sediment trap data from Luostarinen et al. (2020) at GF10 (300 m depth) indicate a MAR and



335 TOC flux comparable to the calculated OCBR. This suggests either efficient preservation of OC settling beyond 300 m or contributions from an additional OC source.

Tidal mixing at the mouths of both Nuup Kangerlua and Ameralik interacts with the sill topography, creating a density gradient that drives intermediate baroclinic circulation (Mortensen et al., 2011; Stuart-Lee et al., 2021). This circulation, characterized by out-fjord flow at depth and in-fjord flow near the surface, reintroduces nutrients to shallower layers, promoting
340 phytoplankton growth in the outer sections of both fjords (Stuart-Lee et al., 2023). In Ameralik, this local productivity likely accounts for the higher pigment and OC content observed in the outer fjord compared to the inner region. However, the absence of similar Chl-a and TOC trends at outer stations GF6 and GF7 in Nuup Kangerlua remains unexplained.

Sørensen et al. (2015) suggested that the observed discrepancy between local primary production and the significantly higher POC export to the sediments in Kobbefjord—a small, glacier-free fjord located between Nuup Kangerlua and Ameralik—
345 could be due to an influx of OC from Nuup Kangerlua. Similarly, part of the OC produced in Nuup Kangerlua may be imported into Ameralik, contributing to increasing TOC and Chl-a content toward Ameralik's mouth. Both fjords exhibit estuarine and intermediate baroclinic circulation (Stuart-Lee et al., 2021), but OC transport efficiency appears greater in Nuup Kangerlua due to strong upwelling driven by subglacial discharge (Mortensen et al., 2014). Consequently, Ameralik may experience net OC import, with deep basin retention and settlement of OC potentially promoting enhanced preservation (Fig. 6). However, a
350 lack of current velocity data for Ameralik limits the ability to fully assess OC transport dynamics.

Still, the observed slightly coarser grain-size fraction in Ameralik's outer and mid fjord stations may signal an input of material from the mouth area as this station is located too far from the glacier input to reveal coarser sediment compared to the inner part of the fjord. Sea Ice and icebergs which could transport coarser material further from the source are absent in the fjord nor is there a debris flow apparent from the grain-size and ^{210}Pb profiles (Fig. A1). The coarser material may therefore originate
355 from the entrance sill indicating a more important deep water inflow compared to Nuup Kangerlua.

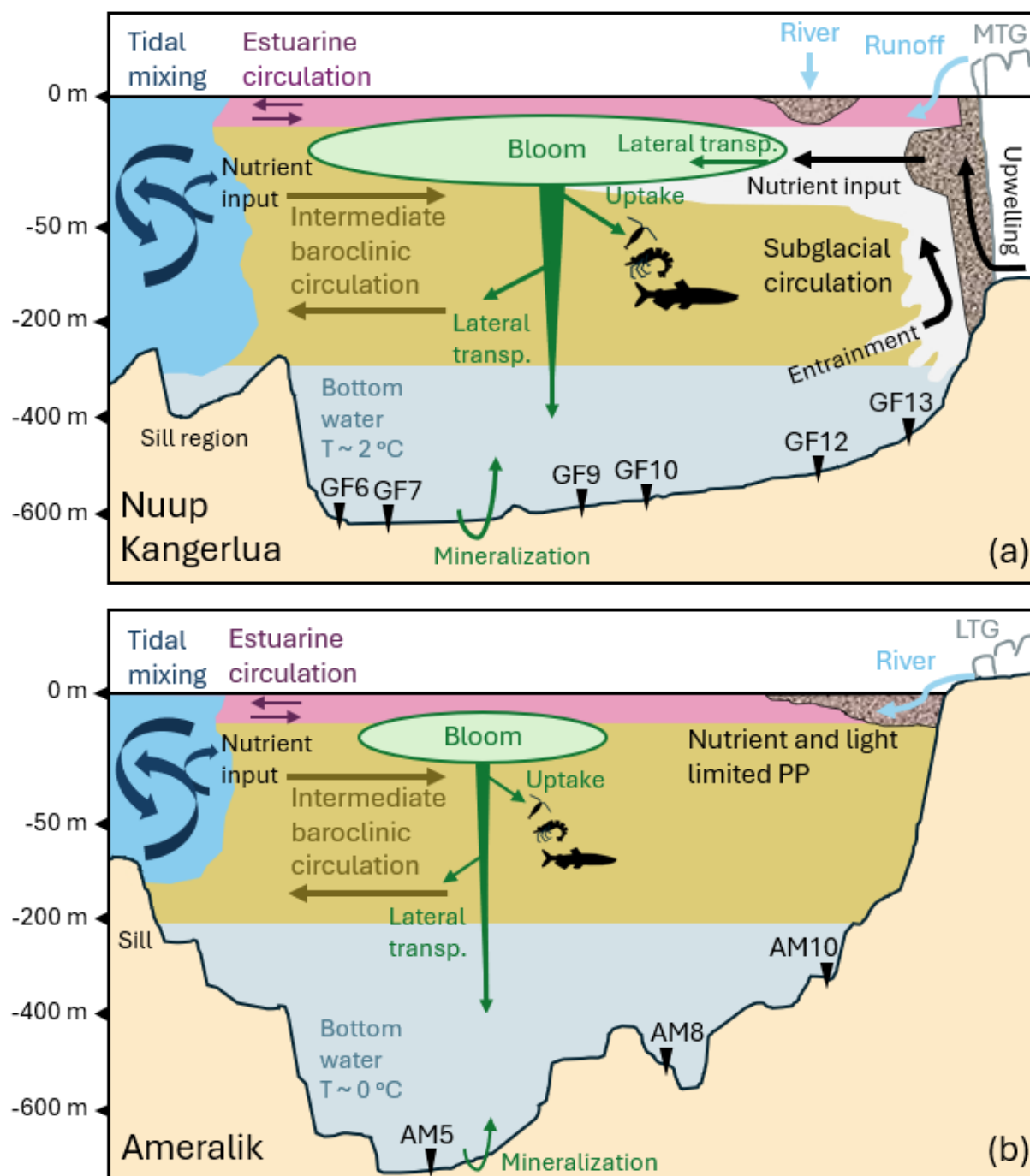


Figure 6: Schematic cross-sectional view of current regime and possible ways of phytoplankton or OC flow during summer in Nuup Kangerlua (A) and Ameralik (B) fjord systems. Tidal mixing above the sill area, estuarine circulation



and intermediate baroclinic circulation occurs in both fjord systems, while the presence of MTGs in Nuup Kangerlua drives subglacial circulation through subglacial discharge. Nutrients are brought to the euphotic zone via tidal mixing and subglacial circulation. Turbid plumes, indicative of suspended sediment and organic matter input from glacier discharge and river runoff, are represented by the shaded brown texture. Green arrows represent phytoplankton or OC transport and remineralization of organic carbon at the sediment-water interface. Station locations are marked along the fjords. The current dynamics illustrated for Nuup Kangerlua are based on Mortensen et al. (2018) and Stuart-Lee et al. (2023), while those for Ameralik are derived from Stuart-Lee et al. (2021; 2023).

4.3 Food web OC flow

360 As both fjords exhibit a high contribution of marine-derived OC compared to other Arctic fjord systems (Fig. 5B), the unexpectedly higher sediment OC content in the basin of Ameralik may be linked to differences in carbon cycling pathways, not only within the sediments, but potentially also above the seafloor. It is possible that the greater biomass and larger size class of phytoplankton in Nuup Kangerlua drive a more extensive and efficient food web (Meire et al., 2023; Stuart-Lee et al., 2023). As a result, a larger portion of OC is channelled into trophic transfer and remineralization, thereby reducing the amount
365 of OC reaching the seafloor compared to Ameralik (Fig 6).

As a consequence of the summer bloom, Nuup Kangerlua has a higher proportion of large herbivorous copepods, while smaller omnivorous species dominate in Ameralik (Stuart-Lee et al., 2024). However, despite these differences in primary producers and composition of zooplankton communities, Stuart-Lee et al. (2024) found no significant difference in zooplankton biomass between the two fjords during the entire melting season. This lack of difference may be influenced by the sampling methods
370 used, as the plankton net in that study was not optimal for capturing larger and more agile zooplankton such as krill (Stuart-Lee et al., 2024), which have been previously recorded in high abundances in the mid and inner part of the fjord (Agersted et al., 2011; Agersted & Nielsen, 2014). Another explanation may be that predation pressure exerts a control on the biomass of the larger and more zooplankton in Nuup Kangerlua (Stuart-Lee et al., 2024). Observations of higher Halibut landings in MTG- compared to LTG-influenced fjords in Greenland (Meire et al., 2017), as well as the importance of MTG fronts as foraging
375 spots for birds and mammals as observed in Svalbard (Lydersen et al., 2014; Urbanski et al., 2017; Vacquié-Garcia et al., 2018; Hamilton et al., 2019), suggest an important transfer of OC through various trophic levels in Nuup Kangerlua. The higher consumption of OC in the water column of Nuup Kangerlua might as such impact the vertical OC transfer to the sediment and result in lower OC content in the sediment of this fjord.



380 4.4 Organic carbon burial rates

Despite the higher organic carbon content observed in the outer and mid part of the LTG-fed fjord, organic carbon burial rates were similar in both fjords. The average OCBR in Ameralik was only slightly, but not significantly, higher ($16.5 \pm 1.7 \text{ gC m}^{-2} \text{ yr}^{-1}$) compared to Nuup Kangerlua ($14.1 \pm 1.6 \text{ gC m}^{-2} \text{ yr}^{-1}$) and fall within the range of Sub-Arctic fjords and Arctic fjords impacted by active glaciers (Włodarska-Kowalczyk et al., 2019). The higher MAR rates in Nuup Kangerlua result from the substantially higher discharge that three MTGs and three LTGs generate compared to the input of a single LTG in Ameralik. Apparently, there is no one-on-one relationship between glacier type and OCBR. Interestingly, despite known differences in pelagic primary production, carbon burial remains similar in both fjords, likely due to limited degradation of organic carbon in Ameralik relative to Nuup Kangerlua. Thus, while the amount and type of glaciers influence both primary production and MAR, the net effect on OCBR appears to be minimal.

390

5 Conclusion

This study provides new insights into carbon burial processes in two southwest Greenland fjords with a different type of glacier influence. Our findings point to complex processes at work regarding carbon burial as our data revealed a different pattern than generally assumed in literature (Hopwood et al., 2020). Our data show that primary production generates most of the organic matter ending up at the seabed sediments in two sub-Arctic fjords with similar metamorphic and igneous catchment geology. Despite the upwelling mechanism in place sustaining more primary production, this process does not seem to induce a higher OC burial in the seabed sediments of a MTG-impacted fjord compared to a LTG-fed fjord. In contrast, this upwelling could be responsible for an export of carbon out the fjord or promoting the transfer of carbon through a more extensive food-web. In that case, MTGs do function as carbon pumps where an important part of the produced OC is stored beyond the fjord basin sediments. However, differences in geomorphology or bottom water characteristics between the two fjords can also override the importance of the subglacial nutrient supply.

Our findings highlight the importance of investigating both the pelagic as benthic compartment of Greenland fjord systems, which are understudied and underrepresented in global carbon budgets compared to other regions. Although this study advances our understanding of the carbon dynamics in Greenland fjords, several unresolved questions remain. For example, differences in diagenetic processes between MTG- and LTG-influenced fjords, along with the role of physical circulation patterns in redistributing OC, require further investigation. Additionally, the potential for complex food webs and higher trophic interactions in MTG fjords to influence carbon sequestration deserves more attention.

Understanding the driving mechanisms of OCBR in fjord systems is essential to predict the impact of climate change on OC sequestration as MTGs evolve to LTGs. The similar OCBR observed between systems suggests that the retreat of MTGs from fjords may not necessarily reduce carbon burial, as new conditions influencing OCBR will emerge. Nevertheless, when assessing the impact of climate change on OC burial budgets, it is crucial to consider the fate of OC produced within the fjord.

410



Appendix A

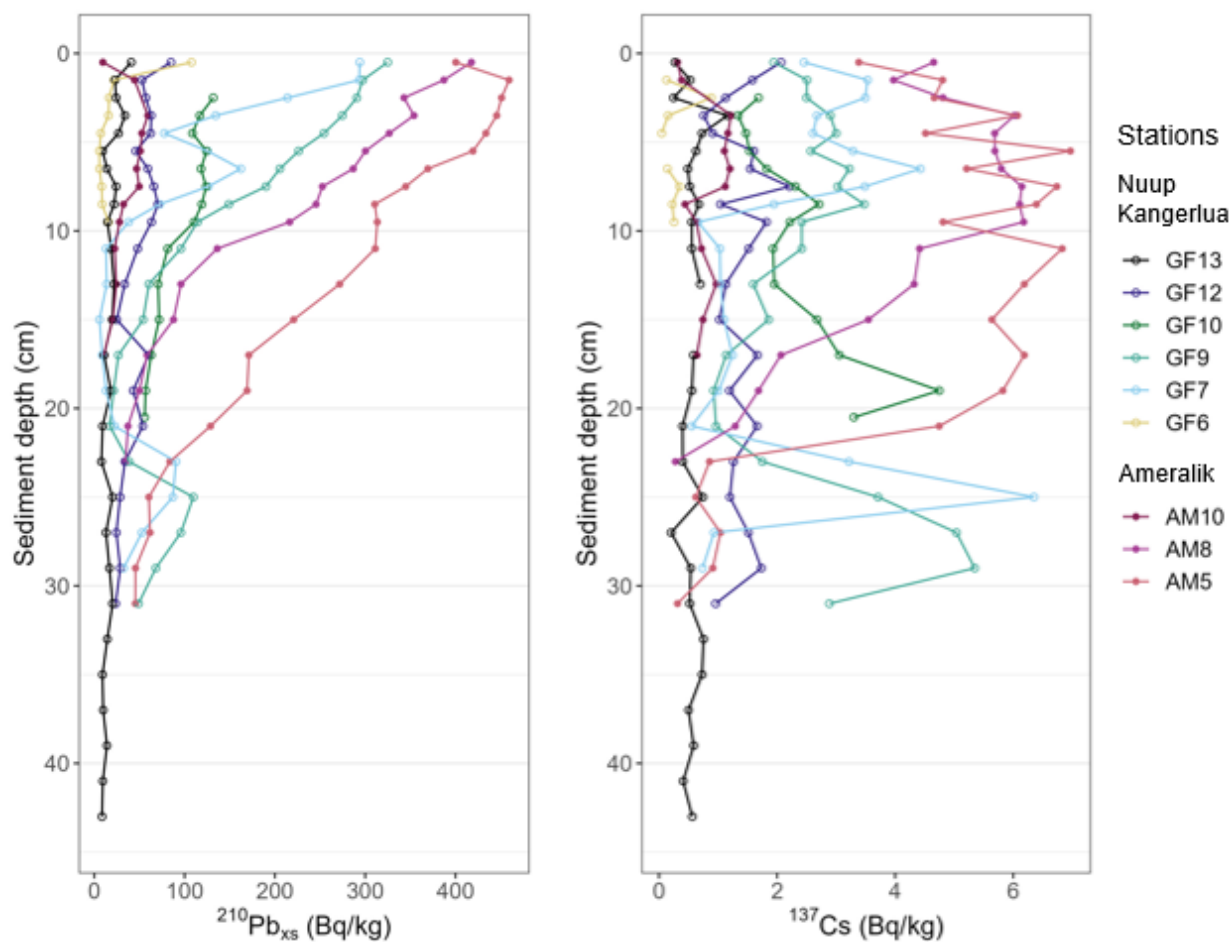


Figure: A1. Excess ^{210}Pb and ^{137}Cs profiles of Nuup Kangerlua stations (GF13, GF12, GF10, GF9, GF7 and GF6) and
 415 Ameralik stations (AM10, AM8 and AM5).

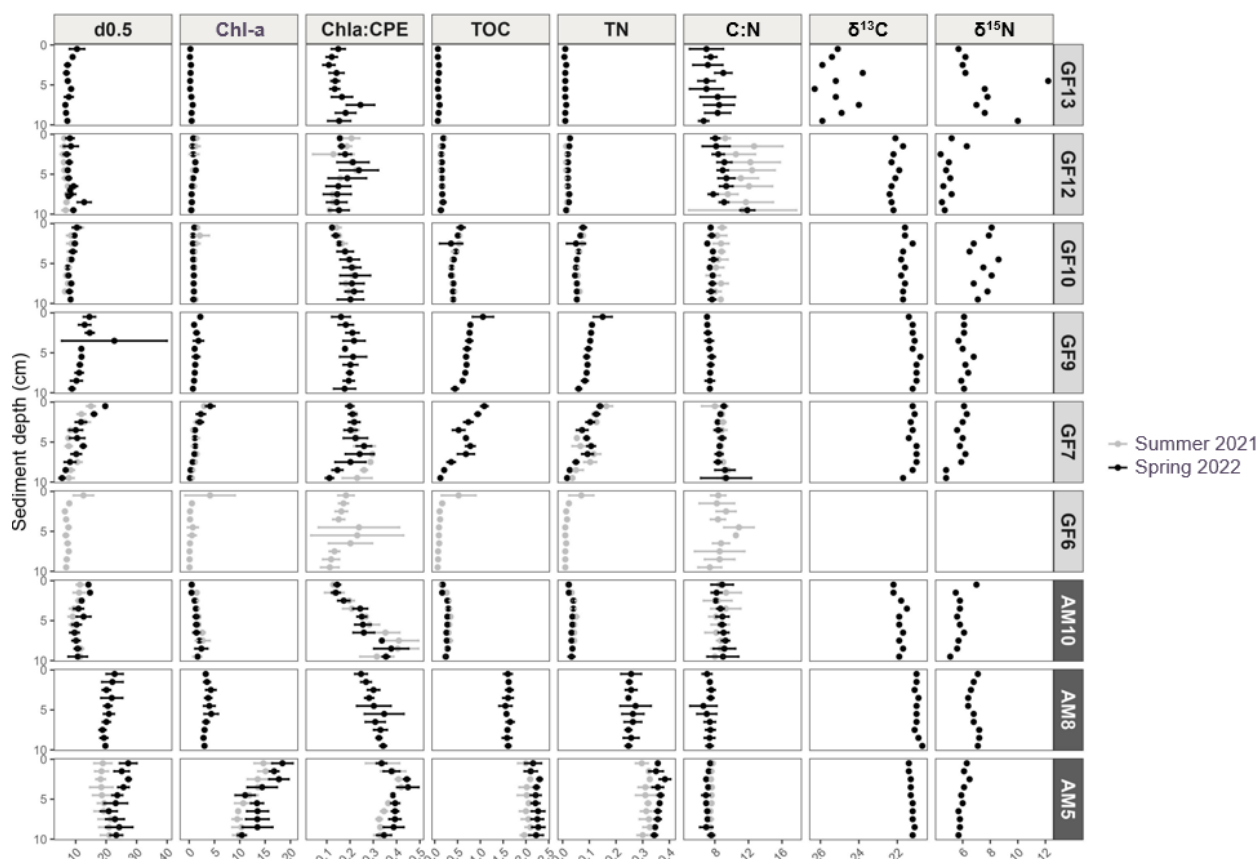


Figure A2: Vertical sediment profiles depicting average median grain size (μm), Chl-a content ($\mu\text{g g}^{-1} \text{DM}$), Chl-a:CPE ratio, TOC and TN (%), and molar C:N ratios, and single core values of $\delta^{13}\text{C}$ (‰), $\delta^{15}\text{N}$ (‰), porosity and dry density (g cm^{-3}) of the upper 10 cm sediment of Nuup Kangerlua (stations GF13, GF12, GF10, GF9, GF7 and GF6) and Ameralik (stations AM10, AM8, AM5). Error bars represent SE ($n = 3$). Orange and black colors represent end of summer 2021 and spring 2022, respectively. Data from the two seasons is available for stations GF12, GF7, AM10 and AM5.

Author contribution

LM, AVR, KS and UB acquired funding for the research project and developed the overall research objectives. LM, MB, UB, AVR, KS and EDB contributed during the field work. SB supervised and carried out lab analyses of Pb^{210} and Cs^{137} . MB conducted formal analysis and AS assisted in MAR calculations and interpretation. MB prepared the original draft and all authors reviewed the manuscript.

Competing interests

The authors declare that they have no conflict of interest.



Acknowledgements

Our sincere thanks to the Greenland Institute of Natural Resources for providing access to lab facilities and the research vessel *Avataq*, as well as accommodations during fieldwork. Special appreciation goes to Captain Peter Rosvig Pedersen and the crew of the *Polar Diver* for their assistance during field sampling. We thank MSc students Charles Makio, Marianne Lollevier and Tran Manh Quan for their contributions to sample processing and preparation. We acknowledge Bart Beuselinck and Bruno Vlaeminck (Ghent University, Marine Biology Research Group) and Peter Van Breughel (NIOZ) for sample analysis. OpenAI's ChatGPT was used to check for grammar and improve the readability of the manuscript.

Financial support

This work is part of the IMAGIN project, funded by Research Foundation-Flanders (FWO) (grant no 3G043120). The research leading to results presented in this publication was carried out with infrastructure funded by EMBRC Belgium - FWO international research infrastructure *1001621N*.

References

- Aciego, S. M., Stevenson, E. I., and Arendt, C. A.: Climate versus geological controls on glacial meltwater micronutrient production in southern Greenland, *Earth And Planetary Science Letters*, 424, 51–58, <https://doi.org/10.1016/j.epsl.2015.05.017>, 2015.
- Agersted, M. D. and Nielsen, T. G.: Krill diversity and population structure along the sub-Arctic Godthåbsfjord, SW Greenland, *Journal Of Plankton Research*, 36, 800–815, <https://doi.org/10.1093/plankt/fbt139>, 2014.
- Agersted, M. D., Nielsen, T. G., Munk, P., Vismann, B., and Arendt, K. E.: The functional biology and trophic role of krill (*Thysanoessa raschii*) in a Greenlandic fjord, *Marine Biology*, 158, 1387–1402, <https://doi.org/10.1007/s00227-011-1657-z>, 2011.
- Appleby, P. G.: Chronostratigraphic techniques in recent sediments, in: *Kluwer Academic Publishers eBooks*, 171–203, https://doi.org/10.1007/0-306-47669-x_9, 2005.
- Bhatia, M. P., Kujawinski, E. B., Das, S. B., Breier, C. F., Henderson, P. B., and Charette, M. A.: Greenland meltwater as a significant and potentially bioavailable source of iron to the ocean, *Nature Geoscience*, 6, 274–278, <https://doi.org/10.1038/ngeo1746>, 2013.
- Bianchi, T. S., Arndt, S., Austin, W. E. N., Benn, D. I., Bertrand, S., Cui, X., Faust, J. C., Kozirowska-Makuch, K., Moy, C. M., Savage, C., Smeaton, C., Smith, R. W., and Syvitski, J.: Fjords as Aquatic Critical Zones (ACZs), *Earth-Science Reviews*, 203, 103145, <https://doi.org/10.1016/j.earscirev.2020.103145>, 2020.
- Brenner, M., Schelske, C. L., and Kenney, W. F.: Inputs of dissolved and particulate ^{226}Ra to lakes and implications for ^{210}Pb dating recent sediments, *Journal Of Paleolimnology*, 32, 53–66, <https://doi.org/10.1023/b:jopl.0000025281.54969.03>, 2004.
- Burdige, D. J.: Preservation of Organic Matter in Marine Sediments: Controls, Mechanisms, and an Imbalance in Sediment Organic Carbon Budgets?, *ChemInform*, 38, <https://doi.org/10.1002/chin.200720266>, 2007.



- 470 Calleja, M. Ll., Kerhervé, P., Bourgeois, S., Kędra, M., Leynaert, A., Devred, E., Babin, M., and Morata, N.: Effects of increase glacier discharge on phytoplankton bloom dynamics and pelagic geochemistry in a high Arctic fjord, *Progress in Oceanography*, 159, 195–210, <https://doi.org/10.1016/j.pocean.2017.07.005>, 2017.
- 475 Catania, G. A., Stearns, L. A., Moon, T. A., Enderlin, E. M., and Jackson, R. H.: Future Evolution of Greenland's Marine-Terminating Outlet Glaciers, *Journal Of Geophysical Research Earth Surface*, 125, <https://doi.org/10.1029/2018jf004873>, 2019.
- Chu, V. W.: Greenland ice sheet hydrology, *Progress in Physical Geography Earth And Environment*, 38, 19–54, <https://doi.org/10.1177/0309133313507075>, 2013.
- 480 Cui, X., Bianchi, T. S., Jaeger, J. M., and Smith, R. W.: Biospheric and petrogenic organic carbon flux along southeast Alaska, *Earth And Planetary Science Letters*, 452, 238–246, <https://doi.org/10.1016/j.epsl.2016.08.002>, 2016a.
- 485 Cui, X., Bianchi, T. S., Savage, C., and Smith, R. W.: Organic carbon burial in fjords: Terrestrial versus marine inputs, *Earth And Planetary Science Letters*, 451, 41–50, <https://doi.org/10.1016/j.epsl.2016.07.003>, 2016b.
- Cutshall, N. H., Larsen, I. L., and Olsen, C. R.: Direct analysis of 210Pb in sediment samples: Self-absorption corrections, *Nuclear Instruments And Methods in Physics Research*, 206, 309–312, [https://doi.org/10.1016/0167-5087\(83\)91273-5](https://doi.org/10.1016/0167-5087(83)91273-5), 1983.
- 490 Faust, J. C. and Knies, J.: Organic matter sources in North Atlantic fjord sediments, *Geochemistry Geophysics Geosystems*, 20, 2872–2885, <https://doi.org/10.1029/2019gc008382>, 2019.
- 495 Faust, J. C., Tessin, A., Fisher, B. J., Zindorf, M., Papadaki, S., Hendry, K. R., Doyle, K. A., and März, C.: Millennial scale persistence of organic carbon bound to iron in Arctic marine sediments, *Nature Communications*, 12, <https://doi.org/10.1038/s41467-020-20550-0>, 2021.
- 500 Faust, J. C., Ascough, P., Hilton, R. G., Stevenson, M. A., Hendry, K. R., and März, C.: New evidence for preservation of contemporary marine organic carbon by iron in Arctic shelf sediments, *Environmental Research Letters*, 18, 014006, <https://doi.org/10.1088/1748-9326/aca780>, 2022.
- 505 Fox, J. and Weisberg, S.: *An R Companion to Applied Regression*, 3rd Edn., Sage, Thousand Oaks, CA, 2019. [Available at: <https://www.john-fox.ca/Companion/>]
- Gilbert, R., Nielsen, N., Möller, H., Desloges, J. R., and Rasch, M.: Glacimarine sedimentation in Kangerdluk (Disko Fjord), West Greenland, in response to a surging glacier, *Marine Geology*, 191, 1–18, [https://doi.org/10.1016/s0025-3227\(02\)00543-1](https://doi.org/10.1016/s0025-3227(02)00543-1), 2002.
- Greene, C. A., Gardner, A. S., Wood, M., and Cuzzone, J. K.: Ubiquitous acceleration in Greenland Ice Sheet calving from 1985 to 2022, *Nature*, 625, 523–528, <https://doi.org/10.1038/s41586-023-06863-2>, 2024.
- 510 Hamilton, C. D., Vacquié-Garcia, J., Kovacs, K. M., Ims, R. A., Kohler, J., and Lydersen, C.: Contrasting changes in space use induced by climate change in two Arctic marine mammal species, *Biology Letters*, 15, 20180834, <https://doi.org/10.1098/rsbl.2018.0834>, 2019.



- 515 Harris, A. J. T. and Elliott, D. A.: Stable Isotope Studies of North American Arctic Populations: A Review, *Open Quaternary*,
5, 11, <https://doi.org/10.5334/oq.67>, 2019.
- Hawkings, J. R., Wadham, J. L., Tranter, M., Raiswell, R., Benning, L. G., Statham, P. J., Tedstone, A., Nienow, P., Lee, K.,
and Telling, J.: Ice sheets as a significant source of highly reactive nanoparticulate iron to the oceans, *Nature Communications*,
5, <https://doi.org/10.1038/ncomms4929>, 2014.
- 520 Hawkings, J. R., Skidmore, M. L., Wadham, J. L., Prisco, J. C., Morton, P. L., Hatton, J. E., Gardner, C. B., Kohler, T. J.,
Stibal, M., Bagshaw, E. A., Steigmeyer, A., Barker, J., Dore, J. E., Lyons, W. B., Tranter, M., and Spencer, R. G. M.: Enhanced
trace element mobilization by Earth's ice sheets, *Proceedings Of The National Academy Of Sciences*, 117, 31648–31659,
<https://doi.org/10.1073/pnas.2014378117>, 2020.
- 525 Herbert, L. C., Zhu, Q., Michaud, A. B., Laufer-Meiser, K., Jones, C. K., Riedinger, N., Stooksbury, Z. S., Aller, R. C.,
Jørgensen, B. B., and Wehrmann, L. M.: Benthic iron flux influenced by climate-sensitive interplay between organic carbon
availability and sedimentation rate in Arctic fjords, *Limnology And Oceanography*, 66, 3374–3392,
<https://doi.org/10.1002/lno.11885>, 2021.
- 530 Hinojosa, J. L., Moy, C. M., Stirling, C. H., Wilson, G. S., and Eglinton, T. I.: Carbon cycling and burial in New Zealand's
fjords, *Geochemistry Geophysics Geosystems*, 15, 4047–4063, <https://doi.org/10.1002/2014gc005433>, 2014.
- 535 Hopwood, M. J., Connelly, D. P., Arendt, K. E., Juul-Pedersen, T., Stinchcombe, M. C., Meire, L., Esposito, M., and Krishna,
R.: Seasonal Changes in Fe along a Glaciated Greenlandic Fjord, *Frontiers in Earth Science*, 4,
<https://doi.org/10.3389/feart.2016.00015>, 2016.
- Hopwood, M. J., Carroll, D., Dunse, T., Hodson, A., Holding, J. M., Iriarte, J. L., Ribeiro, S., Achterberg, E. P., Cantoni, C.,
Carlson, D. F., Chierici, M., Clarke, J. S., Cozzi, S., Fransson, A., Juul-Pedersen, T., Winding, M. H. S., and Meire, L.: Review
540 article: How does glacier discharge affect marine biogeochemistry and primary production in the Arctic?, *The Cryosphere*, 14,
1347–1383, <https://doi.org/10.5194/tc-14-1347-2020>, 2020.
- Juul-Pedersen, T., Arendt, K., Mortensen, J., Blicher, M., Søgaard, D., and Rysgaard, S.: Seasonal and interannual
phytoplankton production in a sub-Arctic tidewater outlet glacier fjord, SW Greenland, *Marine Ecology Progress Series*, 524,
545 27–38, <https://doi.org/10.3354/meps11174>, 2015.
- Kanna, N., Sugiyama, S., Ando, T., Wang, Y., Sakuragi, Y., Hazumi, T., Matsuno, K., Yamaguchi, A., Nishioka, J., and
Yamashita, Y.: Meltwater Discharge From Marine-Terminating Glaciers Drives Biogeochemical Conditions in a Greenlandic
Fjord, *Global Biogeochemical Cycles*, 36, <https://doi.org/10.1029/2022gb007411>, 2022.
- 550 Kassambara, A.: rstatix: Pipe-Friendly Framework for Basic Statistical Tests, R package version 0.7.2, 2023, available at:
<https://rpkgs.datanovia.com/rstatix/>, last access: June 2024.
- King, M. D., Howat, I. M., Candela, S. G., Noh, M. J., Jeong, S., Noël, B. P. Y., Van Den Broeke, M. R., Wouters, B., and
555 Negrete, A.: Dynamic ice loss from the Greenland Ice Sheet driven by sustained glacier retreat, *Communications Earth &
Environment*, 1, <https://doi.org/10.1038/s43247-020-0001-2>, 2020.



- Knies, J. and Martinez, P.: Organic matter sedimentation in the western Barents Sea region: terrestrial and marine contribution based on isotopic composition and organic nitrogen content, *Norw. J. Geol.*, 89, 79–89, 2009.
- 560 Kozirowska, K., Kuliński, K., and Pempkowiak, J.: Sedimentary organic matter in two Spitsbergen fjords: Terrestrial and marine contributions based on carbon and nitrogen contents and stable isotopes composition, *Continental Shelf Research*, 113, 38–46, <https://doi.org/10.1016/j.csr.2015.11.010>, 2015.
- 565 Krause, J., Hopwood, M. J., Höfer, J., Krisch, S., Achterberg, E. P., Alarcón, E., Carroll, D., González, H. E., Juul-Pedersen, T., Liu, T., Lodeiro, P., Meire, L., and Rosing, M. T.: Trace Element (Fe, Co, Ni and Cu) Dynamics Across the Salinity Gradient in Arctic and Antarctic Glacier Fjords, *Frontiers in Earth Science*, 9, <https://doi.org/10.3389/feart.2021.725279>, 2021.
- Kuliński, K., Kędra, M., Legeżyńska, J., Gluchowska, M., and Zaborska, A.: Particulate organic matter sinks and sources in
570 high Arctic fjord, *Journal Of Marine Systems*, 139, 27–37, <https://doi.org/10.1016/j.jmarsys.2014.04.018>, 2014.
- Langen, P. L., Mottram, R. H., Christensen, J. H., Boberg, F., Rodehacke, C. B., Stendel, M., Van As, D., Ahlstrøm, A. P., Mortensen, J., Rysgaard, S., Petersen, D., Svendsen, K. H., Aðalgeirsdóttir, G., and Cappelen, J.: Quantifying Energy and Mass Fluxes Controlling Godthåbsfjord Freshwater Input in a 5-km Simulation (1991–2012)*,+, *Journal Of Climate*, 28, 3694–
575 3713, <https://doi.org/10.1175/jcli-d-14-00271.1>, 2015.
- Laufer-Meiser, K., Michaud, A. B., Maisch, M., Byrne, J. M., Kappler, A., Patterson, M. O., Røy, H., and Jørgensen, B. B.: Potentially bioavailable iron produced through benthic cycling in glaciated Arctic fjords of Svalbard, *Nature Communications*, 12, <https://doi.org/10.1038/s41467-021-21558-w>, 2021.
- 580 Luostarinen, T., Ribeiro, S., Weckström, K., Sejr, M., Meire, L., Tallberg, P., and Heikkilä, M.: An annual cycle of diatom succession in two contrasting Greenlandic fjords: from simple sea-ice indicators to varied seasonal strategists, *Marine Micropaleontology*, 158, 101873, <https://doi.org/10.1016/j.marmicro.2020.101873>, 2020.
- 585 Lydersen, C., Assmy, P., Falk-Petersen, S., Kohler, J., Kovacs, K. M., Reigstad, M., Steen, H., Strøm, H., Sundfjord, A., Varpe, Ø., Walczowski, W., Weslawski, J. M., and Zajaczkowski, M.: The importance of tidewater glaciers for marine mammals and seabirds in Svalbard, Norway, *Journal Of Marine Systems*, 129, 452–471, <https://doi.org/10.1016/j.jmarsys.2013.09.006>, 2013.
- 590 Maslin, M. A. and Swann, G. E. A.: Isotopes In Marine Sediments, in: *Developments in paleoenvironmental research*, 227–290, https://doi.org/10.1007/1-4020-2504-1_06, 2006.
- Meire, L., Søgaard, D. H., Mortensen, J., Meysman, F. J. R., Soetaert, K., Arendt, K. E., Juul-Pedersen, T., Blicher, M. E., and Rysgaard, S.: Glacial meltwater and primary production are drivers of strong CO₂ uptake in fjord and
595 coastal waters adjacent to the Greenland Ice Sheet, *Biogeosciences*, 12, 2347–2363, <https://doi.org/10.5194/bg-12-2347-2015>, 2015.
- Meire, L., Mortensen, J., Meire, P., Juul-Pedersen, T., Sejr, M. K., Rysgaard, S., Nygaard, R., Huybrechts, P., and Meysman, F. J. R.: Marine-terminating glaciers sustain high productivity in Greenland fjords, *Global Change Biology*, 23, 5344–5357,
600 <https://doi.org/10.1111/gcb.13801>, 2017.



- Meire, L., Paulsen, M. L., Meire, P., Rysgaard, S., Hopwood, M. J., Sejr, M. K., Stuart-Lee, A., Sabbe, K., Stock, W., and Mortensen, J.: Glacier retreat alters downstream fjord ecosystem structure and function in Greenland, *Nature Geoscience*, 16, 671–674, <https://doi.org/10.1038/s41561-023-01218-y>, 2023.
- 605 Michaud, A. B., Laufer, K., Findlay, A., Pellerin, A., Antler, G., Turchyn, A. V., Røy, H., Wehrmann, L. M., and Jørgensen, B. B.: Glacial influence on the iron and sulfur cycles in Arctic fjord sediments (Svalbard), *Geochimica Et Cosmochimica Acta*, 280, 423–440, <https://doi.org/10.1016/j.gca.2019.12.033>, 2020.
- 610 Møller, H. S., Jensen, K. G., Kuijpers, A., Aagaard-Sørensen, S., Seidenkrantz, M. -s., Prins, M., Endler, R., and Mikkelsen, N.: Late-Holocene environment and climatic changes in Ameralik Fjord, southwest Greenland: evidence from the sedimentary record, *The Holocene*, 16, 685–695, <https://doi.org/10.1191/0959683606hl963rp>, 2006.
- Moore, O. W., Curti, L., Woulds, C., Bradley, J. A., Babakhani, P., Mills, B. J. W., Homoky, W. B., Xiao, K.-Q., Bray, A. W., 615 Fisher, B. J., Kazemian, M., Kaulich, B., Dale, A. W., and Peacock, C. L.: Long-term organic carbon preservation enhanced by iron and manganese, *Nature*, 621, 312–317, <https://doi.org/10.1038/s41586-023-06325-9>, 2023.
- Mortensen, J., Lennert, K., Bendtsen, J., and Rysgaard, S.: Heat sources for glacial melt in a sub-Arctic fjord (Godthåbsfjord) in contact with the Greenland Ice Sheet, *Journal Of Geophysical Research Atmospheres*, 116, 620 <https://doi.org/10.1029/2010jc006528>, 2011.
- Mortensen, J., Bendtsen, J., Lennert, K., and Rysgaard, S.: Seasonal variability of the circulation system in a west Greenland tidewater outlet glacier fjord, Godthåbsfjord (64°N), *Journal Of Geophysical Research Earth Surface*, 119, 2591–2603, <https://doi.org/10.1002/2014jf003267>, 2014.
- 625 Mortensen, J., Rysgaard, S., Arendt, K. E., Juul-Pedersen, T., Søgaard, D. H., Bendtsen, J., and Meire, L.: Local Coastal Water Masses Control Heat Levels in a West Greenland Tidewater Outlet Glacier Fjord, *Journal Of Geophysical Research Oceans*, 123, 8068–8083, <https://doi.org/10.1029/2018jc014549>, 2018.
- 630 Næraa, T., Kemp, A. I. S., Scherstén, A., Rehnström, E. F., Rosing, M. T., and Whitehouse, M. J.: A lower crustal mafic source for the ca. 2550 Ma Qôrqu Granite Complex in southern West Greenland, *Lithos*, 192–195, 291–304, <https://doi.org/10.1016/j.lithos.2014.02.013>, 2014.
- Ogle, D. H., Doll, J. C., Wheeler, A. P., and Dinno, A.: FSA: Simple Fisheries Stock Assessment Methods, R package version 635 0.9.5, 2023, available at: <https://CRAN.R-project.org/package=FSA>, last access: June 2024.
- Overeem, I., Hudson, B., Welty, E., Mikkelsen, A., Bamber, J., Petersen, D., Lewinter, A. and Hasholt, B.: River inundation suggests ice-sheet runoff retention, *Journal Of Glaciology*, 61, 776–788, <https://doi.org/10.3189/2015jog15j012>, 2015.
- 640 Placitu, S., Van de Velde, S. J., Hylén, A., Hall, P. O. J., Robertson, E. K., Eriksson, M., Leermakers, M., Mehta, N., and Bonneville, S.: Limited Organic Carbon Burial by the Rusty Carbon Sink in Swedish Fjord Sediments, *Journal Of Geophysical Research Biogeosciences*, 129, <https://doi.org/10.1029/2024jg008277>, 2024.



- 645 R Core Team: R: A Language and Environment for Statistical Computing, R Foundation for Statistical Computing, Vienna, Austria, available at: <https://www.R-project.org/>.
- 650 Raiswell, R., Tranter, M., Benning, L. G., Siebert, M., De'ath, R., Huybrechts, P., and Payne, T.: Contributions from glacially derived sediment to the global iron (oxyhydr)oxide cycle: Implications for iron delivery to the oceans, *Geochimica Et Cosmochimica Acta*, 70, 2765–2780, <https://doi.org/10.1016/j.gca.2005.12.027>, 2006.
- Sanchez-Cabeza, J. A. and Ruiz-Fernández, A. C.: 210Pb sediment radiochronology: An integrated formulation and classification of dating models, *Geochimica Et Cosmochimica Acta*, 82, 183–200, <https://doi.org/10.1016/j.gca.2010.12.024>, 2012.
- 655 Smeaton, C. and Austin, W. E. N.: Sources, Sinks, and Subsidies: Terrestrial Carbon Storage in Mid-latitude Fjords, *Journal Of Geophysical Research Biogeosciences*, 122, 2754–2768, <https://doi.org/10.1002/2017jg003952>, 2017.
- Smeaton, C. and Austin, W. E. N.: Where's the Carbon: Exploring the Spatial Heterogeneity of Sedimentary Carbon in Mid-Latitude Fjords, *Frontiers in Earth Science*, 7, <https://doi.org/10.3389/feart.2019.00269>, 2019.
- 660 Smeaton, C., Austin, W. E. N., Davies, A. L., Baltzer, A., Abell, R. E., and Howe, J. A.: Substantial stores of sedimentary carbon held in mid-latitude fjords, *Biogeosciences*, 13, 5771–5787, <https://doi.org/10.5194/bg-13-5771-2016>, 2016.
- Smeaton, C., Yang, H., and Austin, W. E. N.: Carbon burial in the mid-latitude fjords of Scotland, *Marine Geology*, 441, 106618, <https://doi.org/10.1016/j.margeo.2021.106618>, 2021.
- 665 Smith, R. W., Bianchi, T. S., Allison, M., Savage, C., and Galy, V.: High rates of organic carbon burial in fjord sediments globally, *Nature Geoscience*, 8, 450–453, <https://doi.org/10.1038/ngeo2421>, 2015.
- 670 Sørensen, H., Meire, L., Juul-Pedersen, T., De Stigter, H., Meysman, F., Rysgaard, S., Thamdrup, B., and Glud, R.: Seasonal carbon cycling in a Greenlandic fjord: an integrated pelagic and benthic study, *Marine Ecology Progress Series*, 539, 1–17, <https://doi.org/10.3354/meps11503>, 2015.
- Stuart-Lee, A., Møller, E. F., Winding, M., Van Oevelen, D., Hendry, K. R., and Meire, L.: Contrasting copepod community composition in two Greenland fjords with different glacier types, *Journal Of Plankton Research*, <https://doi.org/10.1093/plankt/fbae060>, 2024.
- 675 Stuart-Lee, A. E., Mortensen, J., Van Der Kaaden, A. -s., and Meire, L.: Seasonal Hydrography of Ameralik: A Southwest Greenland Fjord Impacted by a Land-Terminating Glacier, *Journal Of Geophysical Research Oceans*, 126, <https://doi.org/10.1029/2021jc017552>, 2021.
- 680 Stuart-Lee, A. E., Mortensen, J., Juul-Pedersen, T., Middelburg, J. J., Soetaert, K., Hopwood, M. J., Engel, A., and Meire, L.: Influence of glacier type on bloom phenology in two Southwest Greenland fjords, *Estuarine Coastal And Shelf Science*, 284, 108271, <https://doi.org/10.1016/j.ecss.2023.108271>, 2023.
- 685 Thamdrup, B., Glud, R. N., and Hansen, J. W.: Benthic carbon cycling in Young Sound, Northeast Greenland, *Meddelelser Om Grønland Bioscience*, 58, 138–157, <https://doi.org/10.7146/mogbiosci.v58.142646>, 2007.



- Thornton, S. F. and McManus, J.: Application of Organic Carbon and Nitrogen Stable Isotope and C/N Ratios as Source Indicators of Organic Matter Provenance in Estuarine Systems: Evidence from the Tay Estuary, Scotland, *Estuarine Coastal And Shelf Science*, 38, 219–233, <https://doi.org/10.1006/ecss.1994.1015>, 1994.
- Urbanski, J. A., Stempniewicz, L., Węslawski, J. M., Dragańska-Deja, K., Wochna, A., Goc, M., and Iliszko, L.: Subglacial discharges create fluctuating foraging hotspots for sea birds in tidewater glacier bays, *Scientific Reports*, 7, <https://doi.org/10.1038/srep43999>, 2017.
- Vacquié-Garcia, J., Lydersen, C., Ims, R. A., and Kovacs, K. M.: Habitats and movement patterns of white whales *Delphinapterus leucas* in Svalbard, Norway in a changing climate, *Movement Ecology*, 6, <https://doi.org/10.1186/s40462-018-0139-z>, 2018.
- Van As, D., Andersen, M. L., Petersen, D., Fettweis, X., Van Angelen, J. H., Lenaerts, J. T. M., Van Den Broeke, M. R., Lea, J. M., Bøggild, C. E., Ahlstrøm, A. P., and Steffen, K.: Increasing meltwater discharge from the Nuuk region of the Greenland ice sheet and implications for mass balance (1960–2012), *Journal Of Glaciology*, 60, 314–322, <https://doi.org/10.3189/2014jog13j065>, 2014.
- Van Genuchten, C. M., Rosing, M. T., Hopwood, M. J., Liu, T., Krause, J., and Meire, L.: Decoupling of particles and dissolved iron downstream of Greenlandic glacier outflows, *Earth And Planetary Science Letters*, 576, 117234, <https://doi.org/10.1016/j.epsl.2021.117234>, 2021.
- Van Genuchten, C. M., Hopwood, M. J., Liu, T., Krause, J., Achterberg, E. P., Rosing, M. T., and Meire, L.: Solid-phase Mn speciation in suspended particles along meltwater-influenced fjords of West Greenland, *Geochimica Et Cosmochimica Acta*, 326, 180–198, <https://doi.org/10.1016/j.gca.2022.04.003>, 2022.
- Van Heukelem, L. and Thomas, C. S.: Computer-assisted high-performance liquid chromatography method development with applications to the isolation and analysis of phytoplankton pigments, *Journal Of Chromatography A*, 910, 31–49, [https://doi.org/10.1016/s0378-4347\(00\)00603-4](https://doi.org/10.1016/s0378-4347(00)00603-4), 2001.
- Wang, Y., Gélinas, Y., De Vernal, A., Mucci, A. O., Allan, E., Seidenkrantz, M.-S., and Douglas, P. M. J.: High rates of marine organic carbon burial on the southwest Greenland margin induced by Neoglacial advances, *Communications Earth & Environment*, 5, <https://doi.org/10.1038/s43247-024-01508-2>, 2024.
- Watts, E. G., Hylén, A., Hall, P. O. J., Eriksson, M., Robertson, E. K., Kenney, W. F., and Bianchi, T. S.: Burial of Organic Carbon in Swedish Fjord Sediments: Highlighting the Importance of Sediment Accumulation Rate in Relation to Fjord Redox Conditions, *Journal Of Geophysical Research Biogeosciences*, 129, <https://doi.org/10.1029/2023jg007978>, 2024.
- Wehrmann, L. M., Formolo, M. J., Owens, J. D., Raiswell, R., Ferdelman, T. G., Riedinger, N., and Lyons, T. W.: Iron and manganese speciation and cycling in glacially influenced high-latitude fjord sediments (West Spitsbergen, Svalbard): Evidence for a benthic recycling-transport mechanism, *Geochimica Et Cosmochimica Acta*, 141, 628–655, <https://doi.org/10.1016/j.gca.2014.06.007>, 2014.
- Winkelmann, D. and Knies, J.: Recent distribution and accumulation of organic carbon on the continental margin west off Spitsbergen, *Geochemistry Geophysics Geosystems*, 6, <https://doi.org/10.1029/2005gc000916>, 2005.



Włodarska-Kowalczyk, M., Mazurkiewicz, M., Górka, B., Michel, L. N., Jankowska, E., and Zaborska, A.: Organic Carbon
Origin, Benthic Faunal Consumption, and Burial in Sediments of Northern Atlantic and Arctic Fjords (60–81°N), *Journal Of*
735 *Geophysical Research Biogeosciences*, 124, 3737–3751, <https://doi.org/10.1029/2019jg005140>, 2019.

Wright, S. W., and Jeffrey, S. W.: High-resolution HPLC system for chlorophylls and carotenoids of marine phytoplankton,
in: *Phytoplankton pigments in oceanography: Guidelines to modern methods*, edited by: Jeffrey, S. W., Mantoura, R. F. C.,
740 and Wright, S. W., *Monographs on Oceanographic Methodology*, 10, UNESCO Publishing, Paris, pp. 327–341, ISBN 92-3-
103275-5, 1997.

Zaborska, A., Włodarska-Kowalczyk, M., Legeżyńska, J., Jankowska, E., Winogradow, A., and Deja, K.: Sedimentary organic
matter sources, benthic consumption and burial in west Spitsbergen fjords – Signs of maturing of Arctic fjordic systems?,
Journal Of Marine Systems, 180, 112–123, <https://doi.org/10.1016/j.jmarsys.2016.11.005>, 2018.